

# Motion of charged particles near weakly magnetized Schwarzschild black hole

Valeri P. Frolov\* and Andrey A. Shoom†

*Theoretical Physics Institute, University of Alberta, Edmonton, AB, Canada, T6G 2G7*

(Dated: November 26, 2024)

We study motion of a charged particle in the vicinity of a weakly magnetized Schwarzschild black hole and focus on its bounded trajectories lying in the black hole equatorial plane. If the Lorentz force, acting on the particle, is directed outward from the black hole, there exist two qualitatively different types of trajectories, one is a curly motion and another one is a trajectory without curls. We calculated the critical value of the magnetic field for the transition between these two types. If the magnetic field is greater than the critical one, for fixed values of the particle energy and angular momentum, the bounded trajectory has curls. The curls appear as a result of the gravitational drift. The greater the value of the magnetic field, the larger is the number of curls. We constructed an approximate analytical solution for a bounded trajectory and found the gravitational drift velocity of its guiding center.

PACS numbers: 04.70.Bw, 04.70.-s, 04.25.-g

Alberta-Thy-10-10

## I. INTRODUCTION

There exist both theoretical and experimental indications that a magnetic field must be present in the vicinity of black holes. A regular magnetic field can exist near a black hole surrounded by conducting matter (plasma), e.g., if the black hole has an accretion disk. The magnetic field near a stellar mass black hole may contain a contribution from the original magnetic field of the collapsed progenitor star. The dynamo mechanism in the plasma of the accretion disk might generate a regular magnetic field inside the disk. Such a field cannot “cross” the conducting plasma region and is trapped in the vicinity of the black hole (see, e.g., discussion in [1]).

Stellar mass and supermassive black holes often have jets, that is the collimated fluxes of relativistic plasma. It is generally believed that the MHD of the plasma in strong magnetic and gravitational fields of the black holes would allow one to understand formation and energetics of the black holes jets [1]. Magnetic field in the vicinity of the black holes might play an important role in transfer the energy from the accretion disc to jets. Existence of a regular magnetic field near the black holes is also required for the proper collimation of the plasma in the jets.

The simplest mechanism for extraction of the rotation energy from black holes in the presence of magnetic field was proposed by Blandford and Znajek [2]. This mechanism is discussed in detail in the nice book [3]. Interesting results of the numerical simulations, demonstrating jet formation by the plasma in strong magnetic and gravitational fields of the black holes, are presented in [4] (see also references therein). There are some observational evidences of the existence of magnetic field around black holes and its effect on the dynamics of their accretion disks (see, e.g., [5, 6]).

In this paper, we study motion of charged particles in magnetized black holes. To make our presentation more concrete, we shall use the estimations for the magnetic field given in [7]. Namely, the characteristic scales of the magnetic field  $B$  are of the order of  $B_1 \sim 10^8 \text{G}$  near horizon of a stellar mass ( $M_1 \sim 10M_\odot$ ) black hole, and of the order of  $B_2 \sim 10^4 \text{G}$  near horizon of a supermassive ( $M_2 \sim 10^9 M_\odot$ ) black hole. The value of  $B_2$  is also discussed in connection with the Blandford-Znajek mechanism (see, e.g., [2, 3]). It should be emphasized that the aim of the present paper is not to discuss special astrophysical objects, but to study interesting features of the dynamics of a charged particle motion in the presence of both the gravitational field of such black holes and the magnetic field in their vicinity. We use the estimates above to describe only the domain of the physical parameters, which characterize our system, and to define the validity of the adopted approximations.

Let us notice that both the fields  $B_1$  and  $B_2$  are weak in the following sense: The space-time local curvature created by the magnetic field  $B$  is of the order of  $GB^2/c^4$ . It is comparable to the space-time curvature near a black hole of mass  $M$  only if

$$\frac{GB^2}{c^4} \sim \frac{1}{r_g^2} \sim \frac{c^4}{G^2 M^2}. \quad (1)$$

For a black hole of mass  $M$  this condition holds if

$$B \sim B_M = \frac{c^4}{G^{3/2} M_\odot} \left( \frac{M_\odot}{M} \right) \sim 10^{19} (M_\odot/M) \text{G}. \quad (2)$$

Evidently, the quantities  $B_{1,2}$  for both the stellar mass and supermassive black holes presented above are much smaller than the corresponding  $B_M$ . This means that for our problem the field  $B$  can be considered as a test field in the given gravitational background. Such a magnetic field practically does not affect motion of neutral particles.

However, for charged particles, the acceleration induced by the Lorentz force can be large. The acceleration is of the order of  $qB/(mc)$ . Thus, the ‘weakness’ of

\* vfrolov@ualberta.ca

† ashoom@ualberta.ca

the magnetic field  $B$  is compensated by the large value of the charge-to-mass ratio  $q/m$ , which, for example for electrons, is  $e/m_e \approx 5.2728 \times 10^{17} \text{ g}^{-1/2} \text{ cm}^{3/2} \text{ s}^{-1}$ .

In this paper, we consider a Schwarzschild black hole immersed into magnetic field, which is homogeneous at the spatial infinity, where it is directed along the ‘vertical’  $z$ -axis. Close to the black hole this field is strongly affected by its gravity. Such a model is a good approximation for more realistic magnetic fields generated by currents in conducting accretion disk, provided the size of the black hole is much smaller than the size of the disk (see, e.g., discussion in [8]). In our analysis, we shall neglect mutual interaction of charged particles moving around the black hole, i.e., we consider the approximation of a diluted accretion disk. We also restrict ourselves to the motion in the equatorial plane of the black hole, which is orthogonal to the direction of the magnetic field. Similar approximations were considered in the papers [9, 10].

In the presence of the external magnetic field the Lorentz force, acting on a charged particle, depends on the direction of the particle motion. Namely, the presence of the magnetic field breaks the discrete reflection symmetry in the azimuthal direction, so that motion in clockwise and counter-clockwise directions is not equivalent. Many important results on a charged particle motion near a magnetized black hole can be found in the interesting review by Aliev and Gal’tsov [10]. A study of the marginally stable circular orbits around a magnetized Kerr black hole can be found in [11]. Motion of charged particles in the dipolar magnetic field around a static black hole was studied in [12–14], and around a rotating black hole in [15].

To compare the relative strength of the magnetic and gravitational forces acting on a charged particle moving around the black hole let us make the following simple estimations: In a flat space-time (in the absence of gravity) a particle with charge  $q$  and the rest mass  $m$  in the magnetic field  $B$  has the characteristic cyclotron frequency

$$\Omega_c = \frac{|qB|c}{E}, \quad (3)$$

where  $E = \gamma mc^2$  is energy of the particle. Let us compare this frequency with the Keplerian frequency of a particle orbiting a black hole of mass  $M$ ,

$$\Omega_K = \frac{r_g^{1/2} c}{r^{3/2} \sqrt{2}}. \quad (4)$$

Here  $r_g = 2MG/c^2$  is the black hole gravitational radius. For  $r \sim r_g$  and  $\gamma \sim 1$  the ratio of these frequencies  $\Omega_c/\Omega_K$  is of the order of

$$b \equiv \frac{qBMG}{mc^4}. \quad (5)$$

One can use this dimensionless quantity to characterize the relative strength of the magnetic and gravitational

forces acting on a charged particle moving near the black hole. For the motion far from the black hole, the ratio  $\Omega_c/\Omega_K$  contains the additional factor  $(r/r_g)^{3/2}$ .

For a proton of the mass  $m_p$  and the charge  $e$  moving near a magnetized stellar mass or supermassive black hole we have

$$b_1^p = \frac{eB_1GM_1}{m_p c^4} \approx 4.7180 \times 10^7, \quad (6)$$

$$b_2^p = \frac{B_2M_2}{B_1M_1} b_1^p = 10^4 b_1^p, \quad (7)$$

respectively. Both the quantities are large. For electrons their value is larger by the factor  $m_p/m_e \approx 1836$ . This indicates that the effect of the magnetic field on a charged particle motion is not weak. In a general case, such a magnetic field essentially modifies the motion of charged particles. For example, due to this effect the innermost stable circular orbits around a Schwarzschild black hole for proper orientation of the particle rotation are shifted towards its horizon (see, e.g., [9–11, 16]).

The aim of this paper is to study the dynamics of a charged particle moving near magnetized black holes. In particular, we shall demonstrate that in the presence of the magnetic field, there exist two qualitatively different types of the bounded orbits. In the first type, the Keplerian motion is modulated by the cyclotron revolution, so that the particle trajectory has a curly-type structure at small scales. In the second type the particle trajectory has no curls. We study the transition between these two types and calculate the critical value of the corresponding magnetic field. A combined action of gravity and electromagnetism shifts the Keplerian radius and generates the drift of the guiding center of the particle trajectory.

This paper is organized as follows: In Sec. II we present equations of motion of a charged particle moving around a weakly magnetized Schwarzschild black hole. In Sec. III we study motion of a charged particle in a uniform magnetic and weak gravitational fields. Section IV contains an analysis of the effective potential corresponding to a charged particle moving in the equatorial plane of the black hole. In Sec. V we study the innermost stable circular orbits. Section VI contains an analysis of bounded trajectories. In Sec. VII we present an approximate solution for bounded motion of a charged particle. We summarize our results in Section VIII. In this paper we use the sign conventions adopted in [17] and units where  $c = 1$ .

## II. EQUATIONS OF MOTION

### A. Magnetized black hole

We shall study a charged particle motion in the vicinity of a Schwarzschild black hole of mass  $M$  in the presence of an axisymmetric and uniform at the spatial infinity

magnetic field  $B$ . The Schwarzschild metric reads

$$ds^2 = -f dt^2 + f^{-1} dr^2 + r^2 d\omega^2, \quad f = 1 - \frac{r_g}{r}, \quad (8)$$

where  $r_g = 2GM$  and  $d\omega^2 = d\theta^2 + \sin^2 \theta d\phi^2$ . The commuting Killing vectors  $\xi_{(t)} = \partial/\partial t$  and  $\xi_{(\phi)} = \partial/\partial \phi$  generate time translations and rotations around the symmetry axis, respectively.

Because the metric (8) is Ricci flat, the Killing vectors obey the equation

$$\xi^{a;b}{}_{;b} = 0. \quad (9)$$

This equation coincides with the Maxwell equation for a 4-potential  $A^a$  in the Lorentz gauge  $A^a{}_{;a} = 0$ . The special choice

$$A^a = \frac{B}{2} \xi^a_{(\phi)}, \quad (10)$$

corresponds to a test magnetic field, which is homogeneous at the spatial infinity where it has the strength  $B$  (see, e.g., [10, 18]). In what follows, we assume that  $B \geq 0$ . The electric 4-potential (10) is invariant with respect to the isometries corresponding to the Killing vectors, i.e.,

$$(\mathcal{L}_\xi A)_a = A_{a,b} \xi^b + A_b \xi^b{}_{;a} = 0. \quad (11)$$

The magnetic field measured in the rest frame is

$$B_a = -\frac{1}{2} \varepsilon_{abcd} F^{cd} \frac{\xi^b_{(t)}}{|\xi^2_{(t)}|^{1/2}}, \quad \varepsilon_{0123} = \sqrt{-g}. \quad (12)$$

Here  $F_{ab} = A_{b,a} - A_{a,b}$  is the electromagnetic field tensor. The magnetic field corresponding to the 4-potential (10) is

$$B^a \partial_a = B \left(1 - \frac{r_g}{r}\right)^{1/2} \left[ \cos \theta \frac{\partial}{\partial r} - \frac{\sin \theta}{r} \frac{\partial}{\partial \theta} \right]. \quad (13)$$

In the cylindrical coordinates  $(\rho, z, \phi)$  at the spatial infinity it is directed along the  $z$ -axis. The magnetic field (13) coincides with the dipole approximation of the magnetic field of a current loop of the radius  $r = a$  around a Schwarzschild black hole [8]. One can show that this approximation is valid in the region  $r_g < r \ll a$ .

## B. Dynamical equations

Dynamical equation for a charged particle motion is

$$m \dot{u}^a = q F^a_b u^b, \quad (14)$$

where  $u^a$  is the particle 4-velocity,  $u^a u_a = -1$ ,  $q$  and  $m$  are its charge and mass, respectively. Here and in what follows, we denote by the over dot the derivative  $d/d\tau$  with respect to the proper time  $\tau$ . For the motion in the magnetized black hole ((8) and (10)) there exist two

conserved quantities associated with the Killing vectors: the energy  $E > 0$  and the generalized angular momentum  $L \in (-\infty, +\infty)$ ,

$$E \equiv -\xi^a_{(t)} P_a = m \dot{t} \left(1 - \frac{r_g}{r}\right), \quad (15)$$

$$L \equiv \xi^a_{(\phi)} P_a = m \dot{\phi} r^2 \sin^2 \theta + \frac{qB}{2} r^2 \sin^2 \theta. \quad (16)$$

Here  $P_a = m u_a + q A_a$  is the generalized 4-momentum of the particle.

It is easy to check that the  $\theta$ -component of Eq. (14) allows for a solution  $\theta = \pi/2$ . This is a motion in the equatorial plane of the black hole, which is orthogonal to the magnetic field. We restrict ourselves to this type of motion, for which the conserved quantities (15) and (16) are sufficient for the complete integrability of the dynamical equations.

Let us denote

$$\mathcal{E} \equiv \frac{E}{m}, \quad \mathcal{L} \equiv \frac{L}{m}, \quad \mathcal{B} \equiv \frac{qB}{2m}, \quad (17)$$

where  $\mathcal{E}$  and  $\mathcal{L}$  are the specific energy and the specific angular momentum. The  $r$ -component of the dynamical equation (14) for the planar orbits is

$$\ddot{r} = r \left( \frac{\mathcal{L}}{r^2} - \mathcal{B} \right) \left[ \frac{\mathcal{L}}{r^2} \left(1 - \frac{3r_g}{2r}\right) + \mathcal{B} \left(1 - \frac{r_g}{2r}\right) \right] - \frac{r_g}{2r^2}. \quad (18)$$

The first integral of this equation, which follows from Eqs. (15), (16), and (18) is given by

$$\dot{r}^2 = \mathcal{E}^2 - \left(1 - \frac{r_g}{r}\right) \left[ 1 + r^2 \left( \frac{\mathcal{L}}{r^2} - \mathcal{B} \right)^2 \right]. \quad (19)$$

The equations for the azimuthal angle  $\phi$  and the time  $t$  are

$$\dot{\phi} = \frac{\mathcal{L}}{r^2} - \mathcal{B}, \quad \dot{t} = \mathcal{E} \left(1 - \frac{r_g}{r}\right)^{-1}. \quad (20)$$

Equations (18)–(20) are invariant under the following transformations:

$$\mathcal{B} \rightarrow -\mathcal{B}, \quad \mathcal{L} \rightarrow -\mathcal{L}, \quad \phi \rightarrow -\phi. \quad (21)$$

Thus, without loss of the generality, one can assume that the charge  $q$  (and hence  $\mathcal{B}$ ) is positive. For a particle with a negative charge it is sufficient to make the transformation (21).

The geodesic motion in the Schwarzschild space-time (8) is well studied (see, e.g., [17, 19, 20]). Here we study how this motion is modified in the presence of the magnetic field (13). Our problem is reduced to the set of three first-order differential equations (19) and (20) containing two independent parameters  $\mathcal{E}$  and  $\mathcal{L}$ , which are integrals of motion. The solution to the problem depends on the parameters:  $r_0$ ,  $\phi_0$ , and  $t_0$ . They define the initial position of the charged particle. The radial equation (19) can be integrated independently. Substituting its solution into Eq. (20) one can obtain the angular variable  $\phi$  and the time  $t$  by integration.

### III. WEAK GRAVITATIONAL FIELD

#### A. Flat space-time limit

Before we study the motion of a particle near the black hole, it is instructive to consider an approximation of a weak gravitational field. In the absence of gravity, when  $r_g = 0$ , equations (19) and (20) are greatly simplified and take the following form:

$$\dot{r}^2 = \mathcal{E}^2 - 1 - r^2 \left( \frac{\mathcal{L}}{r^2} - \mathcal{B} \right)^2, \quad (22)$$

$$\dot{\phi} = \frac{\mathcal{L}}{r^2} - \mathcal{B}, \quad \dot{t} = \mathcal{E}. \quad (23)$$

The factor  $\mathcal{E}$  in a flat space-time coincides with the Lorentz  $\gamma$ -factor. The solution to equations (22) and (23)

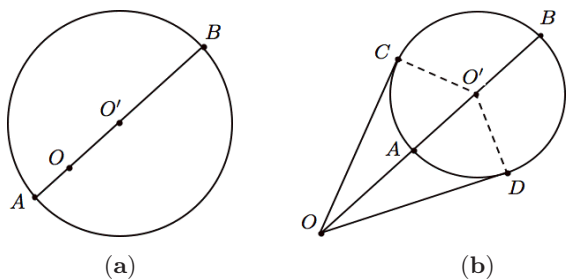


FIG. 1. Motion of a charged particle in a uniform magnetic field in a flat space-time. Points  $A$  and  $B$  define the maximal and the minimal distances of the particle from the coordinate origin  $O$ . (a):  $\mathcal{L} < 0$ . (b):  $\mathcal{L} > 0$ . Points  $C$  and  $D$  are the turning points where  $\dot{\phi} = 0$ .

is well known. The particle moves along a circle of the radius

$$r_c = \sqrt{|\mathcal{L}|/\mathcal{B}}, \quad (24)$$

where  $\mathcal{L} < 0$  is defined with respect to the center of the circle  $O'$ . The corresponding cyclotron frequency (3) and the Lorentz  $\gamma$ -factor are

$$\Omega_c = \frac{2\mathcal{B}}{\mathcal{E}}, \quad \mathcal{E} = \sqrt{1 + 4\mathcal{B}|\mathcal{L}|}. \quad (25)$$

The general solution to equations (22) and (23), which contains two additional constants  $r_0$  and  $\phi_0$ , can be easily obtained by coordinate transformation sending the center of the circle to an arbitrary point  $O$  on the plane  $z = 0$ . Figure 1(a) illustrates the case when the coordinate origin is located inside the circle. More interesting for us case is shown in Fig. 1(b), where the coordinate origin is located outside the circle. For such choice of the coordinates the motion in the  $r$ -direction is bounded, so that  $r_{\min} \leq r \leq r_{\max}$ , and the angle  $\phi$  changes between the two values  $\phi_-$  and  $\phi_+$ . Motions in the  $r$ - and  $\phi$ -direction are correlated and have the same period, so that the resulting trajectory is a circle.

#### B. Approximation of a weak gravitational field

In the presence of the black hole there is a preferable choice of the origin  $O$  of a coordinate system, namely the black hole location. Thus, the symmetry of the flat space-time solution is broken. A black hole also is a source of the additional (gravitational) force acting on the particle. Let us now discuss the motion of the particle in the homogeneous magnetic field, in the approximation when this force is weak.

The corresponding equations can be obtained from equations (18) and (20), assuming that  $r_g/r \ll 1$ . In the leading order we have  $t \approx \mathcal{E}\tau$ , and

$$\ddot{r} = \frac{\mathcal{L}^2}{r^3} - \mathcal{B}^2 r - g, \quad (26)$$

$$\dot{\phi} = \frac{\mathcal{L}}{r^2} - \mathcal{B}. \quad (27)$$

Here  $g = r_g/(2r^2)$  is the Newtonian gravitational force. This force is directed along the radius toward the black hole, and is orthogonal to the magnetic field.

Take a point  $(r_0, \phi_0)$ , such that  $r_g \ll r_0$ , and introduce the local Cartesian coordinates  $(x, y)$  near it, so that  $y$  is directed along the radius vector at the point, and  $x$  is directed ‘‘clockwise’’. For  $x \ll r_0$  and  $y \ll r_0$ , which corresponds to short time intervals  $\Delta\tau$  and strong magnetic field  $\mathcal{B}$ , we have

$$r \approx r_0 + y, \quad \phi \approx \phi_0 - x/r_0. \quad (28)$$

Since  $g$  contains the small factor  $r_g/r_0$ , it is enough to keep the leading term

$$g_0 = \frac{r_g}{2r_0^2}. \quad (29)$$

We substitute expansion (28) into equations (26) and (27), and keep the terms linear in  $x$  and  $y$ .

In the zero order, these equations give

$$\mathcal{L} = \mathcal{B}r_0^2. \quad (30)$$

The first order terms give the following dynamical equations:

$$\ddot{y} = -\Omega^2 y - g_0, \quad (31)$$

$$\dot{x} = \Omega y. \quad (32)$$

Here  $\Omega = 2\mathcal{B} = \Omega_c \mathcal{E}$  is the relativistic cyclotron frequency.

The solution to equations (31) and (32) corresponding to the initial conditions  $x(0) = 0$  and  $y(0) = a - g_0/\Omega^2$  is

$$y(\tau) = a \cos(\Omega\tau) - \frac{g_0}{\Omega^2}, \quad (33)$$

$$x(\tau) = a \sin(\Omega\tau) - (g_0/\Omega)\tau. \quad (34)$$

The line on the  $(x, y)$  plane described by this solution is called a trochoid. For  $g_0 = 0$  this solution describes the motion along a circle with the cyclotron frequency  $\Omega_c$ .

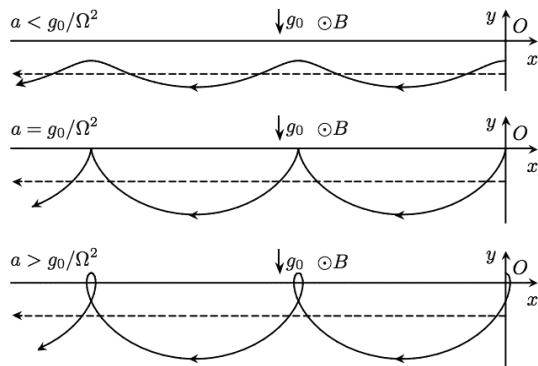


FIG. 2. Motion of a charged particle in the mutually orthogonal uniform magnetic and weak gravitational fields. Dashed line illustrates the motion of the guiding center.

In the presence of gravity the center of the circle moves in the negative  $x$ -direction with the velocity

$$v = r_0 \langle \dot{\phi} \rangle = \frac{g_0}{\Omega}. \quad (35)$$

The velocity  $V$  defined with respect to the rest frame differs by the Lorentz factor  $\dot{t} = \mathcal{E}$ ,

$$V = \frac{v}{\mathcal{E}} = \frac{g_0}{\Omega_c \mathcal{E}^2}. \quad (36)$$

For  $a = g_0/\Omega^2$  the solution takes the form

$$y(\tau) = \frac{g_0}{\Omega^2} [\cos(\Omega\tau) - 1], \quad (37)$$

$$x(\tau) = \frac{g_0}{\Omega^2} [\sin(\Omega\tau) - \Omega\tau]. \quad (38)$$

The line on the  $(x, y)$  plane described by this solution is called a cycloid. It separates two different types of motion, with curls (for  $a > g_0/\Omega^2$ ) and without (for  $a < g_0/\Omega^2$ ) (see Figure 2). Such a curly-type structure is characteristic for a charged particle motion in the presence of both magnetic and non-magnetic forces (see, e.g., [21], Chapter 2).

The obtained solution has a simple interpretation. In a frame moving with the velocity (36) the magnetic field  $B$  ‘generates’ the electric field  $E_y = \gamma V B$ , which is orthogonal to both the field  $B$  and the velocity  $V$ . This electric field, directed along the  $y$ -axis, acts on the charge  $q$  with the force  $qE$ . The velocity  $V$  is defined by the condition, that this force exactly compensates the gravitational force  $mg_0$ . Thus, the motion of a charged particle due to the gravitational force exerted on it in the direction orthogonal to the magnetic field is analogous to the motion of the particle in the constant and mutually orthogonal electric and magnetic fields (see, e.g., [22]).

## IV. CHARGED PARTICLE IN THE SCHWARZSCHILD SPACE-TIME

### A. Dynamical equations

We return to our main problem, motion of a charged particle near a magnetized black hole. It is convenient to introduce the following dimensionless quantities:

$$\mathcal{T} = \frac{t}{r_g}, \quad \rho = \frac{r}{r_g}, \quad \sigma = \frac{\tau}{r_g}, \quad \ell = \frac{\mathcal{L}}{r_g}, \quad (39)$$

and write  $\mathcal{B} = b/r_g$  (see Eqs. (5) and (17)). Then, the dynamical equations (19) and (20) take the following form:

$$\left( \frac{d\rho}{d\sigma} \right)^2 = \mathcal{E}^2 - U, \quad (40)$$

$$\frac{d\phi}{d\sigma} = \frac{\ell}{\rho^2} - b, \quad \frac{d\mathcal{T}}{d\sigma} = \frac{\mathcal{E}\rho}{\rho - 1}. \quad (41)$$

Here

$$U = \left( 1 - \frac{1}{\rho} \right) \left[ 1 + \frac{(\ell - b\rho^2)^2}{\rho^2} \right]. \quad (42)$$

is the effective potential. According to the adopted convention, we have  $b \geq 0$ .

The parameter  $\ell$  can be positive or negative,  $\ell = \pm|\ell|$ . For  $\ell > 0$  (sign +) the Lorentz force, acting on a charged particle, is repulsive, i.e., it is directed outward from the black hole, and for  $\ell < 0$  (sign -) the Lorentz force is attractive, i.e., it is directed toward the black hole<sup>1</sup>.

### B. Effective potential

Let us study properties of the effective potential. We assume that the mass of the black hole and the strength of the magnetic field are fixed. Thus, for a given charged particle the parameter  $b$  is also fixed, and the effective potential is a function of two variables,  $\ell$  and  $\rho$ . We focus on the motion in the black hole exterior, where  $\rho > 1$ . Expression (42) shows that the effective potential is positive in that region. It vanishes at the black hole horizon,  $\rho = 1$ , and grows as  $b^2\rho^2$  for  $\rho \rightarrow +\infty$ . The latter property implies that the particle never reaches the spatial infinity, i.e., its motion is always finite.

To study the characteristic features of  $U$  we use its first and second derivatives

$$U_{,\rho} = \frac{1}{\rho^4} (2b^2\rho^5 - b^2\rho^4 - 2\ell b\rho^2 + \rho^2 - 2\ell^2\rho + 3\ell^2), \quad (43)$$

$$U_{,\rho\rho} = \frac{2}{\rho^5} (b^2\rho^5 - \rho^2 + 2\ell b\rho^2 + 3\ell^2\rho - 6\ell^2). \quad (44)$$

<sup>1</sup> According to the terminology used in the papers [9] and [10], ‘Larmor’ rotation corresponds to the Lorentz force pointing toward the black hole, while ‘anti-Larmor’ rotation corresponds to the Lorentz force pointing in the opposite direction.

Extrema of the effective potential are defined by the equation  $U_{,\rho} = 0$ . The extremal points are the roots of the fifth order in  $\rho$  polynomial in the brackets of expression (43). Such a polynomial may have five real valued roots. We shall show now that because of the specific structure of this polynomial, it has at most two real valued roots in the region  $\rho > 1$ .

For this purpose we write the equation  $U_{,\rho} = 0$  in the following equivalent form:  $P(\rho) = Q(\rho)$ , where

$$P(\rho) = b^2 \rho^4 (2\rho - 1) + \rho^2, \quad (45)$$

$$Q(\rho) = 2\ell b \rho^2 + 2\ell^2 \rho - 3\ell^2. \quad (46)$$

To find a solution to this equation corresponding to the black hole exterior, it is sufficient to find points of the intersection of the curves  $y = P(\rho)$  and  $y = Q(\rho)$  in the interval  $\rho \in [1, \infty)$ . Note that in this interval  $P(\rho)$  is a positive and monotonically growing function, without points of convolution. The second function represents a parabola, which can either intersect the curve  $y = P(\rho)$  at two points, or do not intersect it at all. Note that the case when there is only one intersection in the black hole exterior is excluded for the following reason: In such a case the potential would have only one extremum (maximum or minimum), what is impossible for a positive function vanishing at  $\rho = 0$  and growing at infinity. In the limiting case these curves touch each other at one point, where  $P_{,\rho} = Q_{,\rho}$ . It is easy to check that at this point  $U_{,\rho\rho} = 0$ .

In the former case the intersection of the curves occurs at two points,  $\rho = \rho_{\max}$  and  $\rho = \rho_{\min} > \rho_{\max}$ . The maximum of  $U$  is at  $\rho = \rho_{\max}$ , while its minimum is at  $\rho = \rho_{\min}$ . This means that at  $\rho = \rho_{\min}$  there is a stable circular orbit, while at  $\rho = \rho_{\max}$  there is an unstable one. The condition  $U_{,\rho\rho} = 0$  singles out the innermost (or marginally) stable circular orbit. Figure 3 illustrates the behavior of the effective potential.

Let us define the dimensionless parameter

$$\omega_o^2 = \frac{1}{2} U_{,\rho\rho}(\rho_{\min}) > 0, \quad (47)$$

which is a measure of the curvature of the effective potential at its minimum. It is equal to the square of the frequency of small oscillations about a circular orbit in the radial direction. One can use the equation  $U_{,\rho} = 0$  to express  $\ell b$  in terms of other quantities. Substituting this expression into Eqs. (42) and (47), and eliminating  $\ell$  one obtains the following expression for  $\omega_o$ :

$$\omega_o^2 = \frac{\mathcal{E}_{\min}^2 (\rho_{\min} - 3)}{2\rho_{\min}^2 (\rho_{\min} - 1)^2} + \frac{4b^2}{\rho_{\min}} (\rho_{\min} - 1), \quad (48)$$

where  $\mathcal{E}_{\min}^2 = U(\rho_{\min})$ . This frequency can be written in the dimensional form as follows:

$$\Omega_o^2 = \Omega_K^2 \left(1 - \frac{3r_g}{r_{\min}}\right) + \Omega_c^2 \left(1 - \frac{r_g}{r_{\min}}\right)^3, \quad (49)$$

where the Keplerian frequency  $\Omega_K$  is defined at  $r = r_{\min}$ . Such a relation was derived in [9, 10] (for a more general case see [23]). It illustrates a combination of the

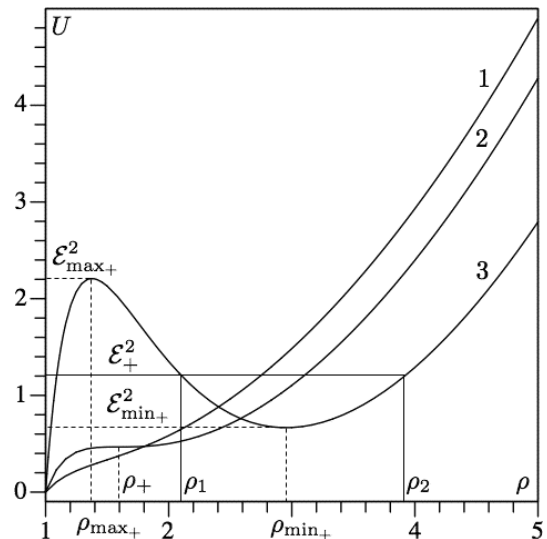


FIG. 3. Effective potential for  $\ell > 0$  and  $b = 1/2$ . Curve 1 corresponds to  $\ell \approx 1.18$ . There are no circular orbits. Curve 2 corresponds to  $\ell \approx 2.07$ . There is the innermost stable circular orbit defined by  $\rho = \rho_+ \approx 1.59$ . Curve 3 corresponds to  $\ell \approx 3.22$ . There are unstable and stable circular orbits corresponding to the minimum and the maximum of the effective potential. For the bounded trajectory corresponding to the energy  $\mathcal{E}_+$  one has  $\rho \in [\rho_1, \rho_2]$ .

cyclotron and Keplerian oscillations due to the gravitational and Lorentz forces acting on a charged particle. In the Schwarzschild space-time circular orbits corresponding to  $r_{\min} > 3r_g$  are always stable, i.e.,  $\Omega_o^2 > 0$ . Marginally stable circular orbits correspond to  $\Omega_o = 0$ .

Let us mention another property of the effective potential, which we shall use later. We denote

$$\rho_* \equiv \sqrt{\ell/b}, \quad (50)$$

then simple calculations give

$$U_{,\rho}(\rho_*) = b/\ell. \quad (51)$$

This means that for bounded orbits and for positive  $\ell$  one has

$$\rho_* > \rho_{\min} \geq \rho_{\max}. \quad (52)$$

## V. THE INNERMOST STABLE CIRCULAR ORBITS

The equations  $U_{,\rho} = 0$  and  $U_{,\rho\rho} = 0$ , which determine the innermost stable circular orbits, can be presented as

<sup>2</sup> The regions of existence and stability of the circular orbits with respect to small oscillations in the radial and vertical ( $\theta$ -) directions where studied in [9].

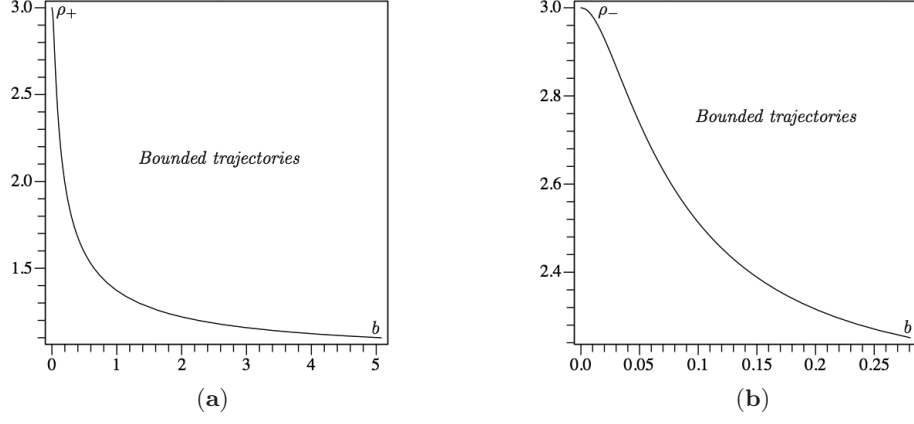


FIG. 4. Dependence of the innermost stable circular orbits  $\rho = \rho_{\pm}$  on  $b$ . For each value of  $b$  one has  $\rho_+ < \rho_-$ . For  $b \rightarrow +\infty$  one has  $\rho_+ \rightarrow 1$  and  $\rho_- \rightarrow (5 + \sqrt{13})/4 \approx 2.15$ .

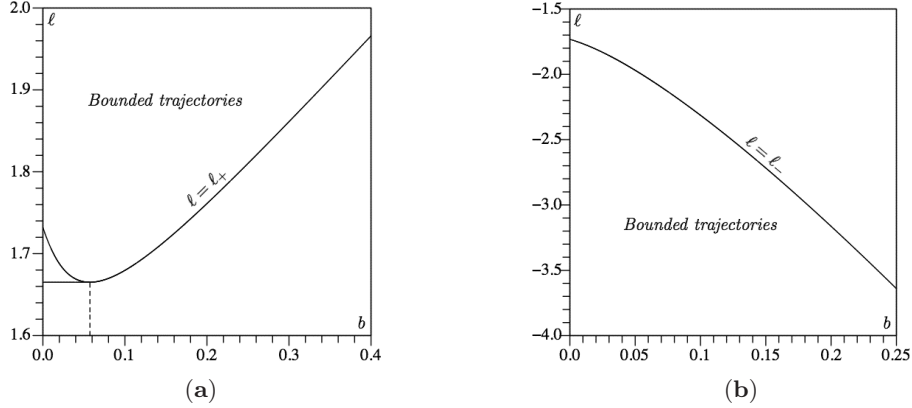


FIG. 5. Angular momenta  $\ell_{\pm}$  for the innermost stable circular orbits as functions of  $b$ . (a):  $\ell > 0$ , the Lorentz force is repulsive. (b):  $\ell < 0$ , the Lorentz force is attractive; the curve  $\ell = \ell_-(b)$  is monotonically decreasing. For  $b = 0$  we have  $\ell_{\pm} = \pm\sqrt{3}$ , what corresponds to a Schwarzschild black hole. For  $b \rightarrow +\infty$  we have  $\ell_{\pm} \rightarrow \pm\infty$ .

follows:

$$b^2 \rho^4 (2\rho - 1) + \rho^2 - 2lb\rho^2 - 2\ell^2\rho + 3\ell^2 = 0, \quad (53)$$

$$b^2 \rho^5 - \rho^2 + 2lb\rho^2 + 3\ell^2\rho - 6\ell^2 = 0. \quad (54)$$

For a given  $b$  these equations allow one to find the parameters  $\rho$  and  $\ell$  for such orbits. As usual for this kind of problems, it is much easier to obtain a solution in an implicit (parametric) form. An addition of equations (53) and (54) let us exclude the terms linear in  $\ell$ . Solving the obtained equation we derive

$$\ell_{\pm} = \pm b \frac{\rho_{\pm}^2 (3\rho_{\pm} - 1)^{1/2}}{(3 - \rho_{\pm})^{1/2}}. \quad (55)$$

The solution exists in the interval  $\rho_{\pm} \in (1/3, 3]$ , where  $\rho_{\pm} = 3$  corresponds to  $b = 0$ . Since we study the black hole exterior, we have  $\rho_{\pm} \in (1, 3]$ . A substitution of

Eq. (55) into either of equations (53) or (54) gives the following equation for  $\rho_{\pm}$ :

$$4\rho_{\pm}^2 - 9\rho_{\pm} + 3 \pm \sqrt{(3\rho_{\pm} - 1)(3 - \rho_{\pm})} - \frac{3 - \rho_{\pm}}{2b^2\rho_{\pm}^2} = 0. \quad (56)$$

This equation allows one to express  $b$  in terms of  $\rho_{\pm}$ ,

$$b = \frac{\sqrt{2}(3 - \rho_{\pm})^{1/2}}{2\rho_{\pm} \left( 4\rho_{\pm}^2 - 9\rho_{\pm} + 3 \pm \sqrt{(3\rho_{\pm} - 1)(3 - \rho_{\pm})} \right)^{1/2}}. \quad (57)$$

Substituting this expression into Eq. (55) we obtain  $\ell_{\pm}$  as a function of  $\rho_{\pm}$ ,

$$\ell_{\pm} = \pm \frac{\rho_{\pm}(3\rho_{\pm} - 1)^{1/2}}{\sqrt{2} \left( 4\rho_{\pm}^2 - 9\rho_{\pm} + 3 \pm \sqrt{(3\rho_{\pm} - 1)(3 - \rho_{\pm})} \right)^{1/2}}. \quad (58)$$

The condition that  $b$  is real does not impose any new restrictions on  $\rho_+$ , so that as above,  $1 < \rho_+ \leq 3$ . For  $\rho_-$  it gives an additional restriction, which is  $(5 + \sqrt{13})/4 < \rho_- \leq 3$ . The position of the innermost stable circular orbit around a Schwarzschild black hole corresponds to  $b = 0$ ,  $\rho_{\pm} = 3$ , and  $\ell_{\pm} = \pm\sqrt{3}$ .

Figure 4 shows plots of  $\rho_{\pm}$  as functions of  $b$ . These plots demonstrate that if the magnetic field increases, the corresponding values of  $\rho_+$  and  $\rho_-$  decrease. For a strong magnetic field and the repulsive Lorentz force, the radius of the innermost stable orbit may be very close to the gravitational radius [11, 13]. Similar plots for  $\ell_{\pm}$  as functions of  $b$  are shown in Figure 5. Let us mention that the curve  $\ell = \ell_+(b)$  has the minimum  $\ell_+ = (3 + \sqrt{5})^2 / (8\sqrt{2 + \sqrt{5}}) \approx 1.67$  at  $b = (\sqrt{5} - 2)^{3/2} / 2 \approx 0.057$ .

In the limit of the strong magnetic field one has

$$\rho_+|_{b \gg 1} = 1 + \frac{1}{b\sqrt{3}} + \mathcal{O}(b^{-2}), \quad (59)$$

$$\rho_-|_{b \gg 1} = \frac{5 + \sqrt{13}}{4} + \frac{41 - 11\sqrt{13}}{36\sqrt{13}b^2} + \mathcal{O}(b^{-4}), \quad (60)$$

$$\ell_+|_{b \gg 1} = b + \sqrt{3} + \mathcal{O}(b^{-1}), \quad (61)$$

$$\ell_-|_{b \gg 1} = -\frac{47 + 13\sqrt{13}}{8}b + \mathcal{O}(b^{-1}). \quad (62)$$

The leading terms in expressions (59) and (60) were derived in [11, 13]. For stable circular orbits one has  $\rho_{\min} > \rho_+$  and  $\ell > \ell_+$ , if the Lorentz force is repulsive, and  $\rho_{\min} > \rho_-$  and  $\ell < \ell_-$ , if the Lorentz force is attractive.

## VI. BOUNDED TRAJECTORIES

If the effective potential is a monotonically growing function of  $\rho$ , a charged particle always starts its motion in the vicinity of the black hole, and after reaching the turning point, it falls down into the black hole. If the effective potential has extrema at  $\rho = \rho_{\max, \min}$ , then for  $\rho < \rho_{\max}$  and  $\mathcal{E}^2 < U(\rho_{\max})$  a charged particle has similar motion. Here we shall not discuss such type of motion. Instead, we focus on study of bounded trajectories. For such trajectories the dimensionless radius  $\rho$  changes between its minimal  $\rho_1$  and maximal  $\rho_2$  values,  $\rho_{\max} \leq \rho_1 \leq \rho_{\min} \leq \rho_2$ , (see Figure 3). These trajectories are more interesting for astrophysical applications, for example for analysis of the motion of particles in the black hole accretion disk. The specific energy  $\mathcal{E}$  for such trajectories obeys the relation

$$\mathcal{E}_{\min} \leq \mathcal{E} \leq \mathcal{E}_{\max}. \quad (63)$$

The radial motion is periodic with the period

$$\Delta\sigma_r = 2 \int_{\rho_1}^{\rho_2} \frac{d\rho}{\sqrt{\mathcal{E}^2 - U(\rho)}}. \quad (64)$$

Let us consider equation (41) for the angular variable  $\phi$

$$\frac{d\phi}{d\sigma} = \frac{\ell}{\rho^2} - b. \quad (65)$$

If the Lorentz force is attractive ( $\ell < 0$ ) the right hand side of this equation is always negative. The corresponding motion of a charged particle is in the clockwise direction. This motion is modulated by oscillations in the radial direction. The corresponding trajectories have no curls. They are similar to bounded trajectories of test particles moving near a Schwarzschild black hole (see, e.g., [19]). The presence of the magnetic field just smoothly deforms them.

From now on we shall focus on more interesting case of the repulsive Lorentz force ( $\ell > 0$ ). In this case there exist two qualitatively different types of the bounded motion. Let  $\rho_1$  and  $\rho_2$  be, as above, the minimal and the maximal values of  $\rho$ . If  $\rho_2 < \rho_*$  the right hand side of Eq. (65) is always positive. The motion has no curls, and  $\phi$  monotonically grows with time. This motion is modulated by oscillations in the radial direction.

For  $\rho_2 > \rho_*$  the motion of the particle is quite different. When the particle moves in the domain  $(\rho_1, \rho_*)$ , we have  $d\phi/d\sigma > 0$ , and the angle  $\phi$  increases, whereas for the motion in the domain  $(\rho_*, \rho_2)$ , we have  $d\phi/d\sigma < 0$ , and the angle  $\phi$  decreases. The corresponding trajectory has curls. Increase of  $\phi$ , corresponding to  $\rho \in [\rho_1, \rho_*)$ , is not exactly compensated by its decrease, corresponding to  $\rho \in (\rho_*, \rho_2]$ . As a result, there is a drift of the particle in the positive  $\phi$ -direction. The critical type of motion corresponding to  $\rho_2 = \rho_*$ , for which the trajectory is similar to a cycloid, is singled out by the condition  $\mathcal{E} = \mathcal{E}_*$ , where

$$\mathcal{E}_* = \sqrt{U(\rho_*)} = \left(1 - \frac{1}{\rho_*}\right)^{1/2}. \quad (66)$$

All the three types of bounded trajectories, with curls, the critical, and without curls, are schematically illustrated in Figure 6. One can see that the bounded trajectories are similar to the trajectories of a charged particle moving in a weak gravitational field discussed in Section III.

For a given  $b$  the motion can be specified by the conserved quantities  $\mathcal{E}$  and  $\ell$ . Different regions in the  $(\mathcal{E}, \ell)$ -plane correspond to different types of motion. Let us discuss this in more detail. We assume that  $\ell > 0$ . The condition  $U_{,\rho} = 0$  determines  $\rho_{\max}$  and  $\rho_{\min}$  as functions of  $\ell$ . Substituting these functions into expression (42) for the effective potential one obtains the corresponding values  $\mathcal{E}_{\max, \min}^2 = U(\rho_{\max, \min}, \ell)$ . For the limiting value  $\ell = \ell_+$ , corresponding to the innermost stable circular orbit, the two curves  $\mathcal{E}_{\max}(\ell)$  and  $\mathcal{E}_{\min}(\ell)$  meet each other. For  $\ell > \ell_+$ , the curve  $\mathcal{E}_{\max}(\ell)$  is always above the curve  $\mathcal{E}_{\min}(\ell)$ . At the points of the extrema of the function  $\mathcal{E}^2(\ell)$  one has

$$\frac{d(\mathcal{E}^2)}{d\ell} = U_{,\ell} = \frac{2b}{\rho^2} \left(1 - \frac{1}{\rho}\right) (\rho_*^2 - \rho^2), \quad (67)$$



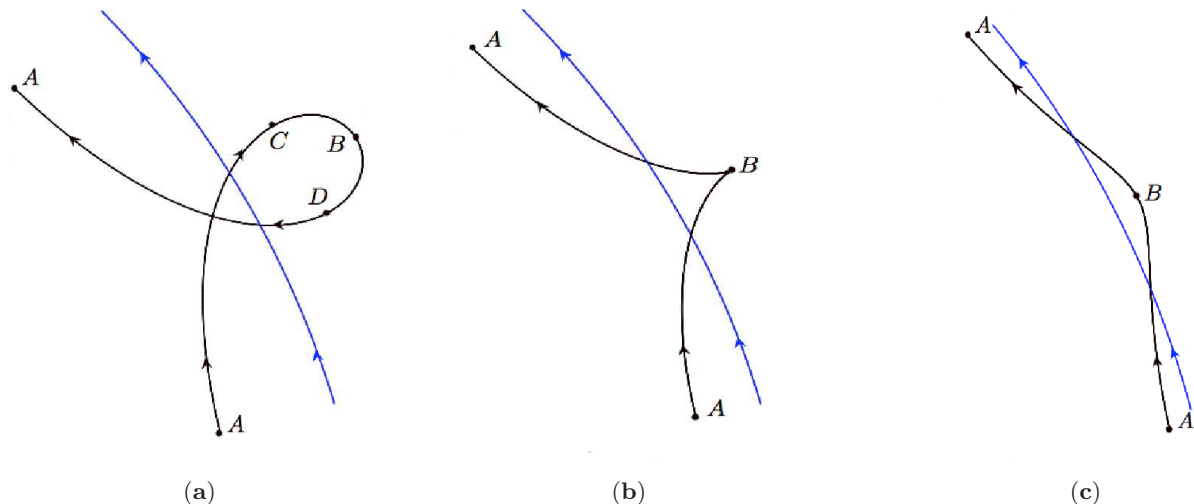


FIG. 6. Types of a bounded trajectory corresponding to  $\ell > 0$ . Arrows illustrate direction of motion of a charged particle. Circular arcs represent the stable circular orbit defined by  $\rho = \rho_{\min,+}$ . (a):  $\mathcal{E}_+ > \mathcal{E}_*$ . Points A's correspond to  $\rho = \rho_1$ , and point B corresponds to  $\rho = \rho_2 > \rho_*$ . Points C and D are turning points, where  $d\phi/d\sigma = 0$ . (b):  $\mathcal{E}_+ = \mathcal{E}_*$ . Points A's correspond to  $\rho = \rho_1$ , and point B is a turning point, which corresponds to  $\rho = \rho_2 = \rho_*$ , where  $d\phi/d\sigma = 0$ . (c):  $\mathcal{E}_+ \in [\mathcal{E}_{\min,+}, \mathcal{E}_*)$ . Points A's correspond to  $\rho = \rho_1$ , and point B corresponds to  $\rho = \rho_2 < \rho_*$ .

where  $\rho = \rho_{\min,\max}$ . Using Eq. (52) we conclude that

$$\frac{d\mathcal{E}_{\max,\min}^2}{d\ell} > 0. \quad (68)$$

Because  $\rho_*$  corresponds to the positive slope of the potential  $U$ , one has  $\mathcal{E}_*(\ell) > \mathcal{E}_{\min}(\ell)$ . Figure 7 illustrates different types of motion for a given magnetic field  $B$ . Two curves on the 'energy-momentum' plane in this plot correspond to the maximum and the minimum of the effective potential. The curve  $\mathcal{E}_+^2 = \mathcal{E}_*^2$  represents the critical energy  $\mathcal{E}_*$  as a function of the angular momentum. The motion for the parameters below this line, in the domain  $I$ , is without curls, while the domain  $II$  corresponds to trajectories with curls.

Such a plot is convenient, for example for the discussion of the following problem: Consider a particle with the parameters  $E$  and  $L$  in the domain  $I$ . Let the particle receives an additional portion of energy  $\Delta E > 0$  and angular momentum  $\Delta L$ . This process moves the point, representing the particle in  $(E, L)$  variables, to a new position. If the point is moved to the domain  $II$ , then the excitation changes the trajectory of the particle, which becomes a curly one.

Using expressions (5), (39), and (66) we can present the critical energy  $\mathcal{E}_*$  in the dimensional form as follows:

$$E_*^2 = m^2 \left( 1 - \sqrt{\frac{qBr_g^2}{2L}} \right) > 0. \quad (69)$$

This expression establishes a relation between the parameters  $E$ ,  $L$ , and  $B$ , corresponding to the critical motion. For given  $B$  and  $L$  the motion is critical if  $E = E_*$ . For

the critical energy  $E_*$  the bounded trajectory has cusps, one of which is illustrated by point  $B$  in Fig. 6(b). One can use Eq. (69) to express the magnetic field  $B$  for the critical motion in terms of the energy  $E$  and the angular momentum  $L$

$$B_* = \frac{2L}{qr_g^2} \left( 1 - \frac{E^2}{m^2} \right)^2, \quad (70)$$

If for fixed values of  $E$  and  $L$  the magnetic field is larger than  $B_*$ , the motion is curly. Thus, keeping the energy and angular momentum of a charged particle fixed, one can change the type of its motion by changing the value of the magnetic field.

## VII. APPROXIMATE SOLUTION FOR BOUNDED MOTION

To analyze properties of bounded trajectories near the minimum of the effective potential  $\mathcal{E}_{\min}^2 = U(\rho_{\min})$  one can expand  $U$  as follows

$$U = \mathcal{E}_{\min}^2 + \omega_o^2(\rho - \rho_{\min})^2 + \dots, \quad (71)$$

where  $\omega_o$  is defined by Eq. (47), and the dots denote the omitted higher order terms of the Taylor expansion. In the linear approximation (71), equation (40) takes the following form:

$$\left( \frac{d\rho}{d\sigma} \right)^2 = \mathcal{E}^2 - \mathcal{E}_{\min}^2 - \omega_o^2(\rho - \rho_{\min})^2. \quad (72)$$

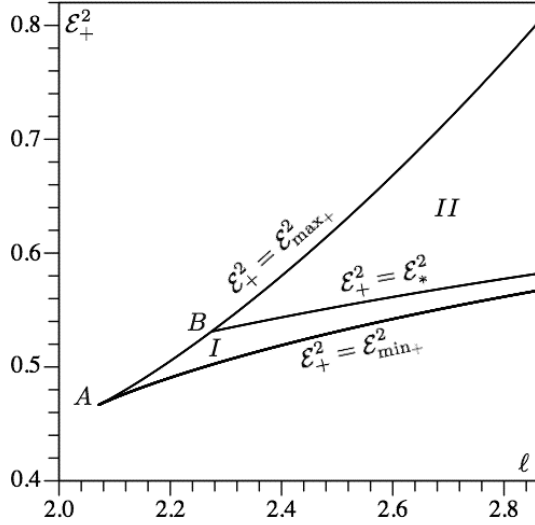


FIG. 7.  $\mathcal{E}_{\max}^2$ ,  $\mathcal{E}_{\min}^2$ , and  $\mathcal{E}_*^2$  as functions of  $\ell$  for a fixed value of  $b$ . Point A, where the curves  $\mathcal{E}_{\max}^2(\ell)$  and  $\mathcal{E}_{\min}^2(\ell)$  join, corresponds to the innermost stable circular orbit. In the domain I between these curves bounded trajectories have no curls. In the domain II between the curves  $\mathcal{E}_*^2$  and  $\mathcal{E}_{\max}^2$  the trajectories are of the curly-type. They degenerate into unstable circular orbit at point B. Bounded motion occurs in the regions I and II. This particular plot is constructed for  $b = 1/2$ . The qualitative behavior for different values of  $b$  is the same.

Analogous expansion of the angular velocity (41) near  $\rho = \rho_{\min}$  gives the linearized equation for  $\phi$

$$\frac{d\phi}{d\sigma} = \beta_0 + \beta_1(\rho - \rho_{\min}), \quad (73)$$

where

$$\beta_0 = \frac{\ell}{\rho_{\min}^2} - b, \quad \beta_1 = -\frac{2\ell}{\rho_{\min}^3}. \quad (74)$$

The validity of the linearized approximation requires that

$$|\rho - \rho_{\min}| \ll \frac{\omega_o^2}{|U_{,\rho\rho}(\rho_{\min})|}, \quad |\rho - \rho_{\min}| \ll \rho_{\min}. \quad (75)$$

We assume that these conditions are satisfied.

Integrating Eqs. (72) and (73) we derive an approximate solution for a bounded trajectory of a charged particle

$$\rho(\sigma) = \rho_{\min} + A \cos(\omega_o \sigma), \quad (76)$$

$$\phi(\sigma) = \beta_0 \sigma + \frac{\beta_1 A}{\omega_o} \sin(\omega_o \sigma), \quad (77)$$

$$A = \frac{\sqrt{\mathcal{E}^2 - \mathcal{E}_{\min}^2}}{\omega_o}, \quad (78)$$

corresponding to the initial conditions  $\rho(0) = \rho_2 = \rho_{\min} + A$  and  $\phi(0) = 0$ . For  $\ell > 0$  this solution describes the motion of a charged particle around the black

hole in the counter-clockwise direction with the average angular velocity equal to  $\beta_0 = \ell \rho_{\min}^{-2} - b$ . This motion is modulated by the radial oscillations of the frequency  $\omega_o$ . Combination of the radial and azimuthal oscillations with the drift results in trajectories, qualitatively similar to those shown in Figs. 2 and 6. The critical solution is singled out by the condition that the trajectory has cusps. It happens for the following amplitude:

$$A = -\frac{\beta_0}{\beta_1} = \frac{\rho_{\min}}{2\rho_*^2}(\rho_*^2 - \rho_{\min}^2). \quad (79)$$

Since  $\rho_* - \rho_{\min} \ll \rho_{\min}$ , this condition implies that  $A \approx \rho_* - \rho_{\min}$  or  $\mathcal{E} \approx \mathcal{E}_*$ , which corresponds to the exactly calculated bounded trajectory with cusps.

The average (drift) velocity of the guiding center in the direction of the increase of  $\phi$  is

$$v = \rho_{\min} \beta_0 = \frac{\ell}{\rho_{\min}} - b \rho_{\min}. \quad (80)$$

The same velocity defined with respect to the time  $t$ , differs from  $v$  by the Lorentz factor  $\dot{t}$  given in (20), and is of the form

$$V = \frac{v}{\dot{t}} = \frac{b(\rho_{\min} - 1)}{\mathcal{E} \rho_{\min}^2}(\rho_*^2 - \rho_{\min}^2). \quad (81)$$

For large values of  $b$  (see Eqs. (6) and (7)) equation  $U_{,\rho} = 0$  can be solved approximately as follows:

$$\rho_{\min}|_{b \gg 1} \approx \rho_* - \frac{1}{8b^2 \rho_*(\rho_* - 1)}. \quad (82)$$

According to this expression, if  $\ell$  is fixed, then  $\rho_{\min}$  is a decreasing function of  $b$ . Thus, strong magnetic field shifts stable circular orbits toward the black hole horizon.

For  $b \gg 1$  in the approximation of a weak gravitational field, that is when  $\rho_{\min} \gg 1$  and  $E \approx mc^2$ , the drift velocity is

$$V \approx \frac{1}{4b\rho_{\min}^2} = \frac{mr_g}{2qBr_o^2} = \frac{g_o}{\Omega_c}. \quad (83)$$

where  $r_o = \rho_{\min} r_g$  and  $g_o = r_g / (2r_o^2)$ . This expression coincides (as expected) with expression (36) for  $\mathcal{E} \approx 1$ .

For  $b \gg 1$  in the approximation of a strong gravitational field, that is  $\rho_{\min} \sim 1$ , one has

$$V \propto r_g \frac{\Omega_K^2}{\Omega_c}, \quad (84)$$

where  $\Omega_K^2$  is the Keplerian frequency (4) calculated for  $r = \rho_{\min} r_g \sim r_g$ . The proportionality constant in (84) depends on the value of the angular momentum  $L$  and is of the order of unity. We see that in both the cases of strong and weak gravitational fields the gravitational drift velocity is proportional to  $B^{-1}$ .

Another quantity which characterizes a bounded trajectory corresponding to the repulsive Lorentz force is the ratio  $N$  of the frequency of the radial oscillations  $\omega_o$

to the average angular velocity  $\beta_o$ . Using Eqs. (48) and (74) we obtain

$$N \equiv \frac{\omega_0}{\beta_o} = \frac{\sqrt{\rho_{\min}^4(3\rho_{\min} - 1) + \rho_*^4(\rho_{\min} - 1)}}{\rho_{\min}^{1/2}(\rho_*^2 - \rho_{\min}^2)}. \quad (85)$$

For  $A > -\beta_o/\beta_1$  this ratio gives the number of curls per one revolution of a particle around the black hole. This ratio depends on  $\rho_{\min}$  and  $\rho_*$ . Using the approximation (82) for  $b \gg 1$  we have

$$N|_{b \gg 1} \approx 8b^2 \rho_*^{3/2} (\rho_* - 1)^{3/2}. \quad (86)$$

Thus, the stronger magnetic field, the greater is the ratio and the number of curls.

### VIII. SUMMARY

In this paper we studied motion of charged particles in the equatorial plane of a weakly magnetized Schwarzschild black hole. We analyzed properties of the corresponding effective potential due to the combined gravitational and Lorentz forces acting on a charged particle. We gave a simple analytical proof that this potential either has two extremal points or none in the black hole exterior. The critical case, when these extrema coincide, determines a position of the innermost stable circular orbit (see also [9–11]). We obtained expressions for the radii and the corresponding angular momenta of the innermost stable orbits in the approximation of the

strong magnetic field ( $b \gg 1$ ). A similar expression for the radii in the limit  $b \rightarrow \infty$  was given before in [11, 13].

In our analysis we mainly focused on the study of bounded trajectories of charged particles. Such trajectories may be considered as an approximation to charged particles motion in the black hole accretion disk, when their mutual interaction is neglected. We constructed an approximate solution to the dynamical equations which represents a bounded trajectory localized near the stable circular orbit.

As a result of our study, we found that if the Lorentz force acting on a charged particle is repulsive, its bounded trajectory can be of two different types: with curls and without them. The critical trajectory, which has cusps, separates these two cases. We calculated the critical value of the magnetic field for the critical trajectory. We calculated also the number of curls per one revolution and found that its maximal value grows with the increase of the magnetic field. Using the approximate solution we found the gravitational drift velocity of the guiding center of a bounded particle trajectory.

### ACKNOWLEDGMENTS

The authors wish to thank the Natural Sciences and Engineering Research Council of Canada for the financial support. One of the authors (V.F.) is grateful to the Killam Trust for its support. He also appreciates fruitful discussions of this work at the meeting Peyresq Physics 15 and is grateful to OLAM, Association pour la Recherche Fondamentale, Brussels, for its financial support.

- 
- [1] B. Punsly, *Black Hole Gravitohydromagnetics* (Springer-Verlag, Berlin, 2001).
  - [2] Blandford R. D., Znajek R. L., *Mon. Not. Roy. Astron. Soc.* **179**, 433 (1977).
  - [3] K. S. Thorne, R. H. Price, and D. A. Macdonald, *Black Holes: The Membrane Paradigm* (Yale University, 1986).
  - [4] S. Koide, K. Shibata, T. Kudoh, and D. L. Meier, *Science* **295**, 1688 (2002).
  - [5] M. de Kool, G. V. Bicknell, and Z. Kuncic, *Publ. Astron. Soc. Aust.* **16**, 225 (1999).
  - [6] J. M. Miller, J. Raymond, A. Fabian, D. Steeghs, J. Homan, C. Reynolds, M. van der Klis, and R. Wijnands, *Nature* **441**, 953 (2006).
  - [7] M. Yu. Piotrovich, N. A. Silant'ev, Yu. N. Gnedin, and T. M. Natsvlshvili, arXiv:1002.4948.
  - [8] J. A. Petterson, *Phys. Rev. D* **10**, 3166 (1974).
  - [9] D. V. Gal'tsov and V. I. Petukhov, *Sov. Phys. JEPT* **47**(3), 419 (1978).
  - [10] A. N. Aliev and D. V. Gal'tsov, *Sov. Phys. Usp.* **32**(1), 75 (1989).
  - [11] A. N. Aliev and N. Özdemir, *Mon. Not. Roy. Astron. Soc.* **336**, 241 (2002).
  - [12] A. R. Prasanna and R. K. Varma, *Pramana* **8**, 229 (1977).
  - [13] G. Preti, *Class. Quantum Grav.* **21**, 3433 (2004).
  - [14] P. Bakala, E. Šrámková, Z. Stuchlík, and G. Török, *Class. Quantum Grav.* **27**, 045001 (2010).
  - [15] A. R. Prasanna and C. V. Vishveshwara, *Pramana* **11**, 359 (1978).
  - [16] R. Znajek, *Nature* **262**, 270 (1976).
  - [17] C. W. Misner, K. S. Thorne and J. A. Wheeler, *Gravitation* (W. H. Freeman and Co., San Francisco, 1973).
  - [18] R. M. Wald, *Phys. Rev. D* **10**, 1680 (1974).
  - [19] S. Chandrasekhar, *The Mathematical Theory of Black Holes* (Clarendon Press, Oxford, England, 1983).
  - [20] V. Frolov and I. Novikov, *Black Hole Physics: Basic Concepts and Recent Developments* (Kluwer Academic Publishers, Dodrecht-Boston-London, 1998), Chapter 14.
  - [21] H. Alfvén, *Cosmical Electrodynamics* (Oxford University Press, Oxford, England, 1963).
  - [22] L. D. Landau and E. M. Lifshitz, *The Classical Theory of Fields* (Pergamon Press, Oxford, England, 1975).
  - [23] A. N. Aliev, in *Proceedings of the Eleventh Marcel Grossmann Meeting on General Relativity, Berlin, 2007*, edited by H Kleinert, R T Jantzen and R Ruffini (Singapore, World Scientific, 2007), p. 1057.